Received 11 January 2024, accepted 11 March 2024, date of publication 13 March 2024, date of current version 21 March 2024.

Digital Object Identifier 10.1109/ACCESS.2024.3377246

RESEARCH ARTICLE

Direct One-Bit DOA Estimation Robust in Presence of Unequal Power Signals

AMIR MASOUD MOLAEI, (Member, IEEE), VINCENT FUSCO, (Fellow, IEEE), AND OKAN YURDUSEVEN, (Senior Member, IEEE)

Institute of Electronics, Communications, and Information Technology, Queen's University Belfast, BT3 9DT Belfast, U.K.

Corresponding author: Amir Masoud Molaei (a.molaei@qub.ac.uk)

This work was supported by the Leverhulme Trust under the Research Leadership Award RL-2019-019.

ABSTRACT Direction-of-arrival (DOA) estimation is a crucial task in wireless communication and radar systems, with applications spanning beamforming, localization, and target tracking. Conventional methods often require high-resolution quantization, imposing challenges and complexities, particularly in large-scale antenna arrays. One-bit DOA estimation has emerged as a groundbreaking alternative, aiming to achieve accurate results without the need for high-resolution measurements. However, state-of-the-art approaches either require reconstruction of an unquantized covariance matrix or sparse signal recovery, or are based on restrictive assumptions such as the equality of power of signal sources. In this paper, a novel approach for direct one-bit DOA estimation is presented, overcoming the limitations of previous methods by introducing a generalized one-bit covariance matrix and smoothing it. Through analytical and numerical analyses, we reveal the shortcomings of the direct application of the one-bit covariance matrix, particularly in scenarios with unequal signal powers. Comparative simulations demonstrate the superiority of the proposed approach, especially in scenarios with significant signal-to-noise ratio differences and a limited number of snapshots.

INDEX TERMS Direction-of-arrival estimation, one-bit measurements, sensor array, sources power.

I. INTRODUCTION

In the ever-evolving landscape of wireless communication and radar systems, direction-of-arrival (DOA) estimation stands as a critical and fundamental task [1], [2], [3]. Accurate DOA estimation plays a pivotal role in a wide range of applications, including beamforming, localization, and target tracking [4], [5], [6]. Over the years, extensive research efforts have been directed towards enhancing the performance of DOA estimation methods. However, one of the persistent challenges in DOA estimation is the need for high-resolution quantization, which often, and especially in emerging large-scale antenna array systems, requires costly and complex hardware setups [7]. The power consumption of analog-to-digital converters (ADCs) increases exponentially with quantization bit number [8]. Therefore, one-bit ADCs, composed of simple comparators, are of great interest in massive multiple-input multiple-output (MIMO) systems due to their minimal circuit power consumption [9], [10].

In response to the aforementioned challenge, a breakthrough has emerged in the form of one-bit DOA estimation, a paradigm-shifting approach that seeks to provide accurate DOA estimation without relying on high-resolution measurements [11], [12], [13]. In [14], an estimator is provided to obtain the normalized scatter matrix of the unquantized data from one-bit samples, which is robust against outliers. In [15], a framework is presented to solve the problem of DOA estimation from one-bit measurements received by a sparse linear array. The performance of such a framework is studied in detail in [11]. Chen et al. [16] modeled the DOA estimation problem of incoherent signals as a binary classification problem and reduced the physical complexity by using sparse arrays. In [17], a gridless approach robust against off-grid errors and sign inconsistency is provided.

All the works mentioned above rely either on the reconstruction of the unquantized covariance matrix or the sparse signal recovery. Huang and Liao [18] showed that the

The associate editor coordinating the review of this manuscript and approving it for publication was Hassan Tariq Chattha.

covariance matrix of one-bit array measurements can be used without mediation for DOA estimation based on subspaces decomposition. However, in modeling and implementation, they have considered the limiting assumption of equal power of signal sources. Such an assumption is not necessarily true in practical applications, because the sources in the environment can be located at different distances from the array or radiate different powers [19].

To overcome the above limitation, in this paper, we first derive the one-bit covariance matrix without restrictions on the power of the sources, generalized one-bit covariance (GOBC) matrix, and express it in terms of the unquantized covariance matrix. Then, with analytical and numerical analyses, we will show how the covariance matrix obtained directly from one-bit measurements may not be reliable against unbalanced signal-to-noise ratios (SNRs). We will also show that such a matrix suffers from the problem of swapping subspaces in conditions of imbalance between sources' powers and limits its use for DOA estimation based on subspaces decomposition techniques. Finally, a solution based on smoothing the GOBC matrix is presented to significantly improve the final results.

The rest of this paper is organized as follows. Section II establishes the data model, providing the main assumptions for subsequent developments. Section III introduces the proposed generalized direct one-bit DOA estimation approach, deriving the GOBC matrix and addressing the limitation of equal power assumptions. Finally, Section IV presents the performance evaluation through computer simulations, comparing the proposed method with existing one-bit approaches.

Notation: Throughout the paper, superscripts $(\cdot)^T$, $(\cdot)^H$ and $(\cdot)^*$ represent the transpose, conjugate transpose and complex conjugate, respectively. The symbols j, $\text{sign}(\cdot)$, $\Re\{\cdot\}$, $\Im\{\cdot\}$, $\mathcal{Q}_1\{z\}$, $\arcsin(\cdot)$, $\mathbb{E}\{\cdot\}$, $\text{diag}(\cdot)$ and $\delta(\cdot)$ denote the imaginary unit, the sign function, the real part and imaginary part, the complex-valued element-wise quantization function, the arcsine function, the expected value operator, the diagonal matrix and the Dirac delta function, respectively. $\mathbf{I}_m$ stands for the $m \times m$ identity matrix.

II. DATA MODEL

Consider K narrowband far-field signals impinging onto a M-element uniform linear array (ULA) from different directions $\{\theta_1, \theta_2, \ldots, \theta_K\}$, where $\theta_k \in [-90°, 90°)$ and $k = 1, 2, \ldots, K$. The inter-element spacing of the array equals half the wavelength ($d = \lambda/2$). The array's data model under one-bit quantization at time $t = 1, 2, \ldots, L$ can be represented as [20]

$$\mathbf{y}(t) \triangleq \mathcal{Q}_1\{\mathbf{x}(t)\} = \mathcal{Q}_1\{\mathbf{A}\mathbf{s}(t) + \mathbf{w}(t)\}, \tag{1}$$

where L is the number of snapshots, and $\mathbf{x}(t) = [x_1(t), x_2(t), \ldots, x_M(t)]^T \in \mathbb{C}^{M\times 1}$ and $\mathbf{y}(t) = [y_1(t), y_2(t), \ldots, y_M(t)]^T \in \mathbb{C}^{M\times 1}$ denote unquantized array observations and one-bit array measurements, respectively. $\mathbf{s}(t) = [s_1(t), s_2(t), \ldots, s_K(t)]^T \in \mathbb{C}^{K\times 1}$ and $\mathbf{w}(t) = [w_1(t), w_2(t), \ldots, w_M(t)]^T \in \mathbb{C}^{M\times 1}$ represent signal and noise vectors, respectively, which are assumed to be uncorrelated and modeled as zero-mean circular complex Gaussian random processes. The power of the k-th signal source and the noise power are denoted by σ_k^2 and σ_w^2, respectively. The steering vector of the steering matrix $\mathbf{A} = [\mathbf{a}(\theta_1), \mathbf{a}(\theta_2), \ldots, \mathbf{a}(\theta_K)] \in \mathbb{C}^{M\times K}$ [21] is expressed as $\mathbf{a}(\theta_k) = [a_1(\theta_k), a_2(\theta_k), \ldots, a_M(\theta_k)]^T \in \mathbb{C}^{M\times 1}$ with

$$a_m(\theta_k) = e^{j\tau_{m,k}}, \tag{2}$$

where $\tau_{m,k} = -2\pi(m-1)d\sin\theta_k/\lambda$ denotes the propagation time delay between the first sensor (reference) and the m-th one, and $m = 1, 2, \ldots, M$. In (1), $\mathcal{Q}_1\{z\}$ is defined as [22]

$$\mathcal{Q}_1\{z\} = \frac{1}{\sqrt{2}}\left(\text{sign}(\Re\{z\}) + j\text{sign}(\Im\{z\})\right). \tag{3}$$

III. GENERALIZED DIRECT ONE-BIT DOA ESTIMATION

The arcsine law [14], [23] states that if $\mathbf{x}(t)$ is a circularly-symmetric complex Gaussian vector with zero mean and covariance $\mathbf{R_x} = \mathbb{E}\{\mathbf{x}(t)\mathbf{x}^H(t)\}$ (consistent with the assumptions of the data model in Section II), then the covariance matrix $\mathbf{R_y} = \mathbb{E}\{\mathbf{y}(t)\mathbf{y}^H(t)\}$ corresponding to the signal $\mathbf{y}(t)$ (see (1)) is related to $\mathbf{R_x}$ as follows:

$$\mathbf{R_y} = \frac{2}{\pi}\arcsin\left(\bar{\mathbf{R}}_\mathbf{x}\right), \tag{4}$$

where $\bar{\mathbf{R}}_\mathbf{x} \triangleq \mathbf{D}^{-1/2}\mathbf{R_x}\mathbf{D}^{-1/2}$ is the normalized covariance of the unquantized samples $\mathbf{x}(t)$, $\mathbf{D} \triangleq \text{diag}([\mathbf{R_x}]_{1,1}, [\mathbf{R_x}]_{2,2}, \ldots, [\mathbf{R_x}]_{m,m})$ and $\arcsin(z) = \arcsin(\Re\{z\}) + j\arcsin(\Im\{z\})$.

According to (1) and (2), and the uncorrelation of signals and noise, the (m, m')-th entry of the matrix $\mathbf{R_x}$ is obtained from the following equation:

$$\begin{aligned}[\mathbf{R_x}]_{m,m'} &= \mathbb{E}\left\{x_m(t)x_{m'}^*(t)\right\} \\ &= \mathbb{E}\left\{\left[\sum_{k=1}^{K} a_m(\theta_k)s_k(t) + w_m(t)\right]\right. \\ &\qquad \left.\times\left[\sum_{k=1}^{K} a_{m'}^*(\theta_k)s_k^*(t) + w_{m'}^*(t)\right]\right\} \\ &= \sum_{k=1}^{K} a_m(\theta_k)a_{m'}^*(\theta_k)\sigma_k^2 + \sigma_\text{w}^2\delta(m-m'),\end{aligned} \tag{5}$$

where $\sigma_k^2 = \mathbb{E}\{s_k(t)s_k^*(t)\}$, $\sigma_w^2 = \mathbb{E}\{w_m(t)w_m^*(t)\}$ and $m' = 1, 2, \ldots, M$. Therefore, $\mathbf{D} = P\mathbf{I}_M$, where $P \triangleq \sum_{k=1}^{K}\sigma_k^2 + \sigma_\text{w}^2$, and as a result we have

$$[\bar{\mathbf{R}}_\mathbf{x}]_{m,m'} = \frac{\sum_{k=1}^{K} a_m(\theta_k)a_{m'}^*(\theta_k)\sigma_k^2 + \sigma_\text{w}^2\delta(m-m')}{\sum_{k=1}^{K}\sigma_k^2 + \sigma_\text{w}^2}$$

$$= \begin{cases} 1, & m = m', \\ \dfrac{\sum_{k=1}^{K} a_m(\theta_k) a_{m'}^*(\theta_k) \sigma_k^2}{\sum_{k=1}^{K} \sigma_k^2 + \sigma_w^2} = \dfrac{\sum_{k=1}^{K} a_m(\theta_k) a_{m'}^*(\theta_k) \chi_k}{\sum_{k=1}^{K} \chi_k + 1}, & m \neq m', \end{cases} \quad (6)$$

where $\chi_k \triangleq \sigma_k^2 / \sigma_w^2$ represents the SNR of the k-th signal. According to (2) and (6), we have

$$\Re\left\{\left[\bar{\mathbf{R}}_\mathbf{x}\right]_{m,m'}\right\} = \frac{\sum_{k=1}^{K} \Re\left\{e^{j\left(\tau_{m,k} - \tau_{m',k}\right)}\right\} \chi_k}{\sum_{k=1}^{K} \chi_k + 1} = \frac{\sum_{k=1}^{K} \cos\left(\tau_{m,k} - \tau_{m',k}\right) \chi_k}{\sum_{k=1}^{K} \chi_k + 1}, \quad m \neq m'. \quad (7)$$

By using the generalized triangle inequality [24], it can be easily proved that

$$\left|\sum_{k=1}^{K} \cos\left(\tau_{m,k} - \tau_{m',k}\right) \chi_k\right| \leq \sum_{k=1}^{K} \left|\cos\left(\tau_{m,k} - \tau_{m',k}\right)\right| \chi_k \leq \sum_{k=1}^{K} \chi_k. \quad (8)$$

Therefore, considering (7) and (8), we can conclude that

$$\left|\Re\left\{\left[\bar{\mathbf{R}}_\mathbf{x}\right]_{m,m'}\right\}\right| = \frac{\left|\sum_{k=1}^{K} \cos\left(\tau_{m,k} - \tau_{m',k}\right) \chi_k\right|}{\sum_{k=1}^{K} \chi_k + 1} \leq \frac{\sum_{k=1}^{K} \chi_k}{\sum_{k=1}^{K} \chi_k + 1}, \quad m \neq m'. \quad (9)$$

Similarly, for the imaginary part, we can write

$$\left|\Im\left\{\left[\bar{\mathbf{R}}_\mathbf{x}\right]_{m,m'}\right\}\right| = \frac{\left|\sum_{k=1}^{K} \sin\left(\tau_{m,k} - \tau_{m',k}\right) \chi_k\right|}{\sum_{k=1}^{K} \chi_k + 1} \leq \frac{\sum_{k=1}^{K} \chi_k}{\sum_{k=1}^{K} \chi_k + 1}, \quad m \neq m'. \quad (10)$$

Since in practice, always $\sum_{k=1}^{K} \chi_k > 0$, then $\left|\Re\left\{\left[\bar{\mathbf{R}}_\mathbf{x}\right]_{m,m'}\right\}\right| \leq 1$ and $\left|\Im\left\{\left[\bar{\mathbf{R}}_\mathbf{x}\right]_{m,m'}\right\}\right| \leq 1$. $\left|\Re\left\{\left[\bar{\mathbf{R}}_\mathbf{x}\right]_{m,m'}\right\}\right| = \left|\Im\left\{\left[\bar{\mathbf{R}}_\mathbf{x}\right]_{m,m'}\right\}\right| = 1$, for $m \neq m'$, occurs only when a noise-free scenario is considered, or the signal power is infinite. Therefore, in practice, it can be said that for $m \neq m'$, $\left|\Re\left\{\left[\bar{\mathbf{R}}_\mathbf{x}\right]_{m,m'}\right\}\right| < 1$ and $\left|\Im\left\{\left[\bar{\mathbf{R}}_\mathbf{x}\right]_{m,m'}\right\}\right| < 1$. Also, (9) and (10) indicate that the lower the sum of SNRs, the smaller the upper bounds of $\left|\Re\left\{\left[\bar{\mathbf{R}}_\mathbf{x}\right]_{m,m'}\right\}\right|$ and $\left|\Im\left\{\left[\bar{\mathbf{R}}_\mathbf{x}\right]_{m,m'}\right\}\right|$ (go towards zero). For example, suppose two signals with DOAs of $-40°$ and $10°$ and with SNRs of χ_1 and $\chi_1 - 5$ dB, respectively, impinge onto a 10-element array. The values of $R_{m'} \triangleq \left|\Re\left\{\left[\bar{\mathbf{R}}_\mathbf{x}\right]_{1,m'}\right\}\right|$ and $I_{m'} \triangleq \left|\Im\left\{\left[\bar{\mathbf{R}}_\mathbf{x}\right]_{1,m'}\right\}\right|$ for different χ_1s are illustrated in Fig. 1. The curves in Fig. 1 confirm the theoretical findings derived above.

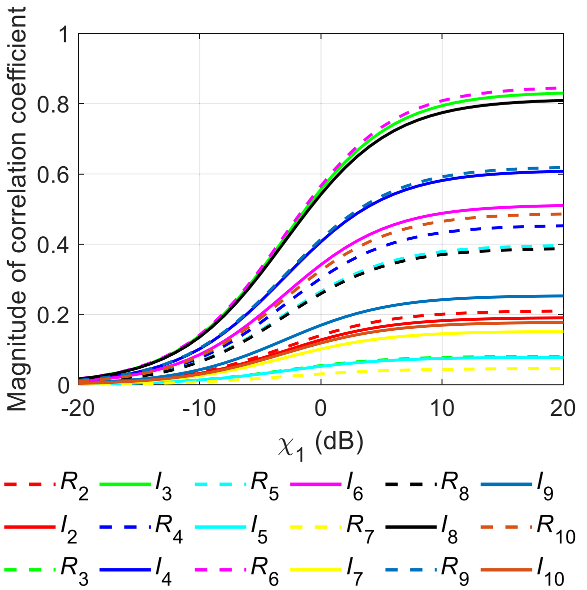

FIGURE 1. The magnitude of the real and imaginary parts of the correlation coefficient versus different SNRs.

According to the derived bounds in the previous paragraph, the convergence of Taylor series expansions $\arcsin\left(\Re\left\{\left[\bar{\mathbf{R}}_\mathbf{x}\right]_{m,m'}\right\}\right)$ and $\arcsin\left(\Im\left\{\left[\bar{\mathbf{R}}_\mathbf{x}\right]_{m,m'}\right\}\right)$ are guaranteed [25]. In addition, if $\left|\Re\left\{\left[\bar{\mathbf{R}}_\mathbf{x}\right]_{m,m'}\right\}\right|$ and $\left|\Im\left\{\left[\bar{\mathbf{R}}_\mathbf{x}\right]_{m,m'}\right\}\right|$ are small enough, or equivalently, the sum of the SNRs is sufficiently low, the high-order terms of the arcsin expansion can be omitted and according to (4) we write:

$$\left[\mathbf{R}_\mathbf{y}\right]_{m,m'} = \frac{2}{\pi} \arcsin\left(\left[\bar{\mathbf{R}}_\mathbf{x}\right]_{m,m'}\right) \simeq \frac{2}{\pi} \left[\bar{\mathbf{R}}_\mathbf{x}\right]_{m,m'}, \quad m \neq m'. \quad (11)$$

For $m = m'$, since according to (6) and (4), $\left[\bar{\mathbf{R}}_\mathbf{x}\right]_{m,m'} = \left[\mathbf{R}_\mathbf{y}\right]_{m,m'} = 1$, therefore, the above approximation cannot be applied. However, by rewriting (11) into the form (12)

$$\mathbf{R}_\mathbf{y} - \mathbf{I}_M \simeq \frac{2}{\pi}\left(\bar{\mathbf{R}}_\mathbf{x} - \mathbf{I}_M\right), \quad (12)$$

the following closed form (GOBC matrix) can be obtained:

$$\mathbf{R}_\mathbf{y} \simeq \frac{2}{\pi} \bar{\mathbf{R}}_\mathbf{x} + 0.36 \mathbf{I}_M. \quad (13)$$

Let $\mathbf{v} \in \mathbb{C}^{M\times 1}$ be an eigenvector of $\mathbf{R_x}$ corresponding to an eigenvalue λ, then $\mathbf{R_x v} = \lambda \mathbf{v}$ [26]. Therefore, we can write

$$\begin{aligned}\mathbf{R_y v} &\simeq \left(\frac{2}{\pi}\bar{\mathbf{R}}_\mathbf{x} + 0.36\mathbf{I}_M\right)\mathbf{v}\\ &= \left(\frac{2}{\pi}P^{-1/2}\mathbf{I}_M\mathbf{R_x}P^{-1/2}\mathbf{I}_M + 0.36\mathbf{I}_M\right)\mathbf{v}\\ &= \frac{2}{\pi P}\mathbf{R_x v} + 0.36\mathbf{I}_M\mathbf{v} = \frac{2}{\pi P}\lambda\mathbf{v} + 0.36\mathbf{v}\\ &= \left(\frac{2}{\pi P}\lambda + 0.36\right)\mathbf{v}. \end{aligned} \tag{14}$$

From (14), we can conclude that although the eigenvalues of $\mathbf{R_y}$ are obtained by scaling the eigenvalues of $\mathbf{R_x}$ by $2/(\pi P)$ and adding 0.36, the eigenvectors of $\mathbf{R_y}$ and $\mathbf{R_x}$ are almost the same. As a result, for DOA estimation methods based on eigenvectors, such as subspace techniques, the GOBC matrix can be used directly, considering applied approximations. However, considering that measurements $\mathbf{y}(t)$, unlike measurements $\mathbf{x}(t)$, are limited to only four values $(\pm 1 \pm j)/\sqrt{2}$ (according to (1) and (3)), the data of $\mathbf{R_y}$, which in practice are estimated as $\hat{\mathbf{R}}_\mathbf{y} = \sum_{t=1}^{L}\mathbf{y}(t)\mathbf{y}^H(t)/L$, experience faster (high-frequency) changes, especially when the number of snapshots is small. The results of the simulations that will be presented in Section IV show that the direct application of the GOBC matrix may lead to the phenomenon of swapping subspaces under conditions where the powers of the received signals are too unbalanced. In particular, the greater the differences of signals' powers, the greater the difference between the eigenvalues corresponding to the signals (i.e. $\lambda_1, \lambda_2, \ldots, \lambda_K$); and the eigenvalues of the weaker signals are closer to the $\lambda_{K+1}, \lambda_{K+2}, \ldots, \lambda_M$, where $\lambda_1 \geq \lambda_2 \geq \ldots \geq \lambda_M$. This leads to inter-subspace leakage [27], in which a share of the true signal subspace resides in the estimated noise subspace. Therefore, some steering vectors may not be completely orthogonal to the noise subspace. Ultimately, this may cause DOAs to be incorrectly estimated. Note that this becomes more acute when the estimation relies on low-resolution measurements (quantization). To overcome this problem, we apply to the data $\hat{\mathbf{R}}_\mathbf{y}$, before subspace decomposition, a smoothing operation that acts as a low-frequency filtering. This preprocessing step reduces the impact of high-frequency changes in the data, making the subsequent subspace decomposition more robust and accurate. After applying the filtering, an estimate of the smoothed GOBC matrix $\hat{\mathbf{R}}_{\mathbf{y}\_\mathrm{Smoothed}}$ is obtained. For this purpose, various smoothing filters such as moving mean, moving median, Gaussian, etc. [28] can be employed.

DOAs can be estimated by the following spectral search function:

$$\hat{\theta}_k = \arg\max_{\theta} \underbrace{\left[\mathbf{a}^H(\theta)\mathbf{Q}_{\mathrm{n\_Smoothed}}\mathbf{Q}^H_{\mathrm{n\_Smoothed}}\mathbf{a}^H(\theta)\right]^{-1}}_{f(\theta)}, \tag{15}$$

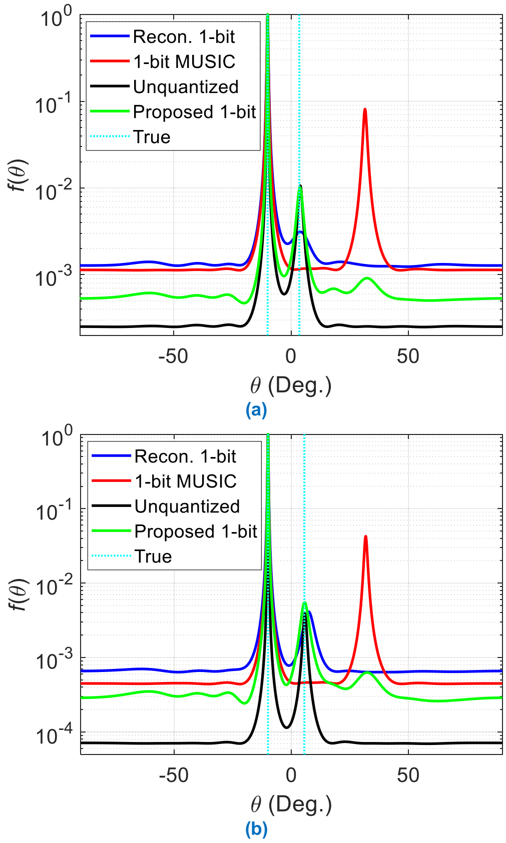

FIGURE 2. Comparison of the estimated spatial spectra of various methods when the SNRs of the signals are different; (a) $\theta_2 = 3.5°$, (b) $\theta_2 = 5.5°$.

where

$$\hat{\mathbf{R}}_{\mathbf{y}\_\mathrm{Smoothed}} = \mathbf{Q}_{\mathrm{s\_Smoothed}}\mathbf{\Lambda}_{\mathrm{s\_Smoothed}}\mathbf{Q}^H_{\mathrm{s\_Smoothed}} + \mathbf{Q}_{\mathrm{n\_Smoothed}}\mathbf{\Lambda}_{\mathrm{n\_Smoothed}}\mathbf{Q}^H_{\mathrm{n\_Smoothed}}, \tag{16}$$

where $\mathbf{Q}_{\mathrm{s\_Smoothed}}$, spanning the signal subspace of $\hat{\mathbf{R}}_{\mathbf{y}\_\mathrm{Smoothed}}$, consists of the eigenvectors related to the diagonal elements of $\mathbf{\Lambda}_{\mathrm{s\_Smoothed}}$. Similarly, $\mathbf{Q}_{\mathrm{n\_Smoothed}}$ consists of the eigenvectors related to the diagonal elements of $\mathbf{\Lambda}_{\mathrm{n\_Smoothed}}$, which spans the noise subspace of $\hat{\mathbf{R}}_{\mathbf{y}\_\mathrm{Smoothed}}$.

IV. PERFORMANCE EVALUATION AND DISCUSSION

In this section, the results of computer simulations to verify the performance of the proposed approach (generalized direct one-bit DOA estimation) are presented along with the discussion. Also, comparisons are made with one-bit multiple signal classification (MUSIC) with covariance matrix reconstruction [23], MUSIC with unquantized measurements [29] and one-bit MUSIC algorithm [18]. A 10-element ULA is considered. The signals and noise are independent and identically distributed complex Gaussian processes with zero mean. In all simulations, $\sigma_\mathrm{w}^2 = 1$. Unless otherwise specified, $L = 1000$, and two narrowband signals impinge on the array from $\theta_1 = -10°$ and $\theta_2 = 3.5°$. In all methods, the step size of the angle search is 0.1°. To smooth the

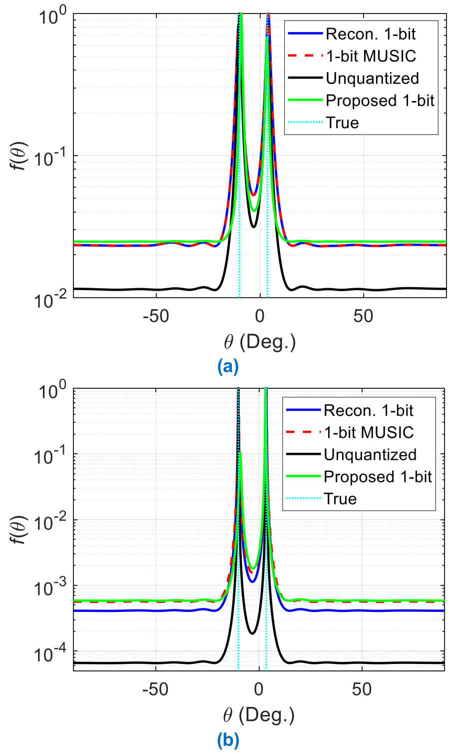

FIGURE 3. Comparison of the estimated spatial spectra of various methods when the SNRs of the signals are the same; (a) $\chi_1 = \chi_2 = -10$ dB. Note that the same performance of the blue and red spectra in the case where the SNRs of the signals are equal and low is consistent with the analysis of [18], (b) $\chi_1 = \chi_2 = 10$ dB.

GOBC matrix, we have used the Gaussian filter [30], which provided the best performance in our experiments. All results are obtained from averaging $N_T = 1000$ Monte Carlo runs. To evaluate the accuracy of the estimates, the root-mean-square error (RMSE) criterion with the definition of

$$\mathrm{RMSE} = \sqrt{\sum_{k=1}^{K} \sum_{i=1}^{N_T} \left(\hat{\theta}_{k,i} - \theta_k\right)^2 \Big/ N_T K}$$

is used, where $\hat{\theta}_{k,i}$ represents an estimate of θ_k in the i-th trial [31].

Fig. 2(a) shows the normalized estimated spatial spectra of various methods when the SNRs of the signals are different (the first is 10 dB and the second is -10 dB). As can be seen, the output of the proposed approach (green diagram) has a better resolution than other one-bit approaches, although logically the best resolution belongs to unquantized MUSIC (black diagram). More noteworthy is the performance of the one-bit MUSIC method (red diagram). It can be seen that the estimated DOA of the second signal with lower SNR has a significant error (see right peak). Fig. 2(b) shows the simulation outputs when the second source is moved to 5.5° (keeping other parameters constant). Again, the peaks of all the methods are around the correct DOAs, except for the one-bit MUSIC method. The estimated DOA of the second source, like Fig. 2(a), is about 31.5°. In other words, in the case of the one-bit MUSIC method, although the original DOA of the second source is changed, there is no change in the estimated DOA. Now let us consider Fig. 3. Fig. 3(a) and Fig. 3(b) show the outputs of the mode where the SNRs of both signals are $\chi_1 = \chi_2 = -10$ dB and $\chi_1 = \chi_2 = 10$ dB, respectively. This time, the one-bit MUSIC method works correctly (whether the SNR is low or the SNR is high). Considering the above, it can be concluded that the one-bit MUSIC method [18], which is a direct estimation approach from one-bit data, fails when the SNRs are different. In Section III, it was stated that the reason for this issue is the problem of swapping subspaces. To confirm this, we have demonstrated three different cases in Fig. 4. In all three cases, $\chi_1 = 10$ dB and $\chi_2 = -10$ dB. Fig. 5 shows the allocation of signal and noise subspaces in the

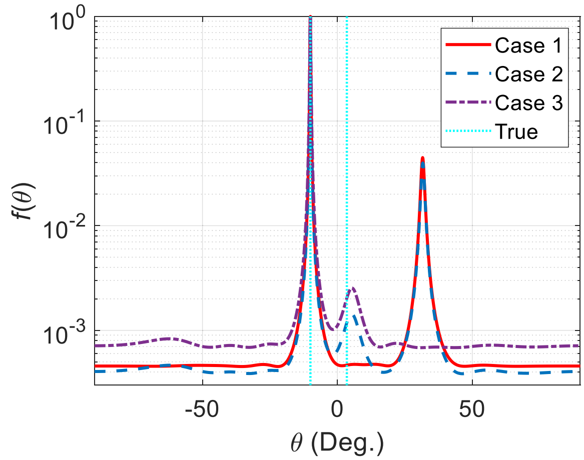

FIGURE 4. Spatial spectra of one-bit MUSIC algorithm [18] in three different cases. $\chi_1 = 10$ dB and $\chi_2 = -10$ dB.

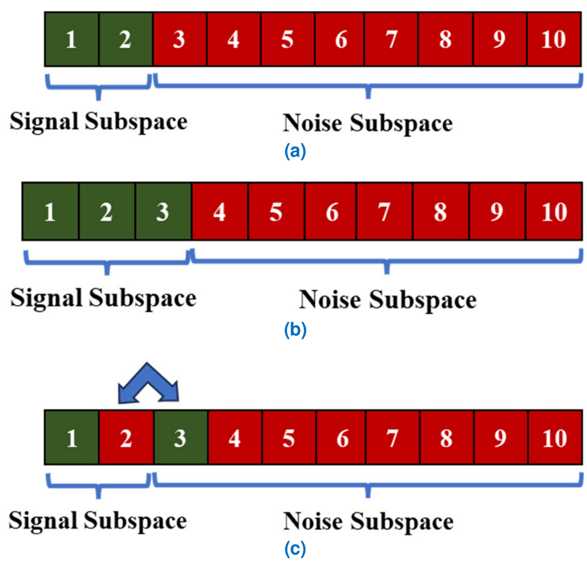

FIGURE 5. Allocation of signal and noise subspaces in one-bit MUSIC algorithm [18] corresponding to Fig. 4. The eigenvectors 1 to 10 corresponding to the largest to smallest eigenvalues are sorted; (a) Case 1, (b) Case 2, (c) Case 3.

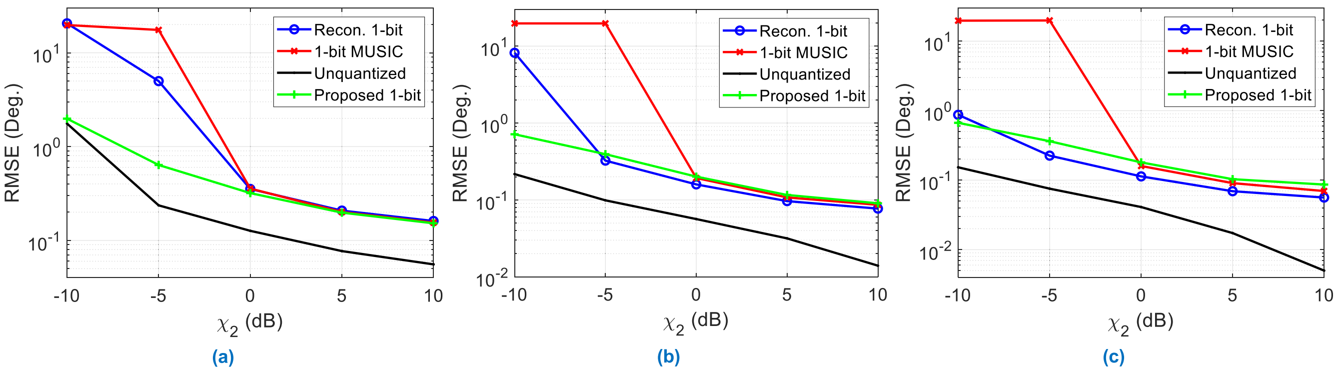

FIGURE 6. Comparison of RMSEs of various methods versus the SNR of the second source when $\chi_1 = 10$ dB; (a) $L = 100$, (b) $L = 500$, (c) $L = 1000$.

corresponding cases. Case 1 represents the normal state of decomposition of signal and noise subspaces, where the two eigenvectors corresponding to the largest eigenvalues of the covariance matrix in [18] constitute the signal subspace, and the remaining eigenvectors form the noise subspace [18]. In this case, only one of the peaks (corresponding to the stronger signal) is correct (see Fig. 4). In Case 2, although there are only two sources, three eigenvectors corresponding to three larger eigenvalues are considered as the signal subspace. The result is that three peaks can be identified in Fig. 4, the two on the left side are correct and the right peak does not correspond to any signal. Finally, considering Case 3, we find that the problem is in the eigendecomposition of the covariance matrix in the approach [18] so that since the SNR of the second signal is significantly different from the SNR of the first one, the eigenvector corresponding to the weaker signal is swapped with the strongest component of the noise subspace. As we showed in Fig. 1, the proposed approach does not suffer from such a practical problem.

Now, the estimation accuracy in various methods is compared. In this experiment, the SNR of the first source is assumed to be fixed and equal to 10 dB. By changing the SNR of the second source from -10 to 10 dB, the RMSE values for different numbers of snapshots are calculated in Fig. 6. From the results, it can be seen that when the SNR difference between two sources is more than about 10 dB, the proposed one-bit approach performs much better than other one-bit methods, especially when the number of snapshots is less. This is consistent with the explanation in Section III. Also, when the SNRs of the sources are close to each other, the proposed approach exhibits competitive performance. In addition, according to the theoretical analyzes related to correlation coefficient and power in Section III, when the sum of SNRs is lower (compared to the case where the sum of SNRs is higher), we expect the performance of the proposed approach to be closer to the outputs of unquantized data. The results of Fig. 6 confirm this. It is quite natural that the lowest RMSEs always belong to the results obtained by unquantized data (with infinite precision). For further investigation, in Fig. 7, a 3-D surface plot of the performance of each method is extracted. In Fig. 7, in addition to changing

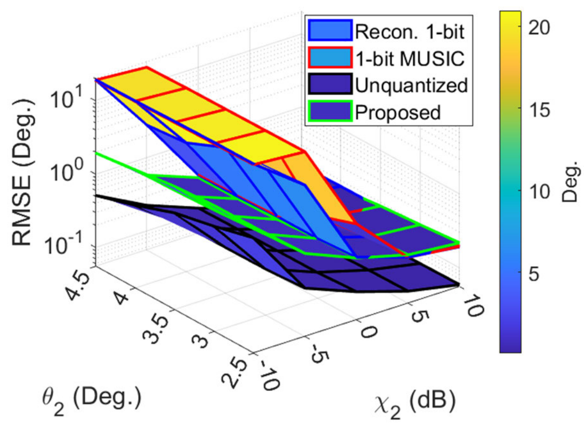

FIGURE 7. 3-D surface plot of the performance of various methods. $L = 100$. Different methods are distinguished by different edge line colors. Faces and colorbar are color-coded according to the RMSE range.

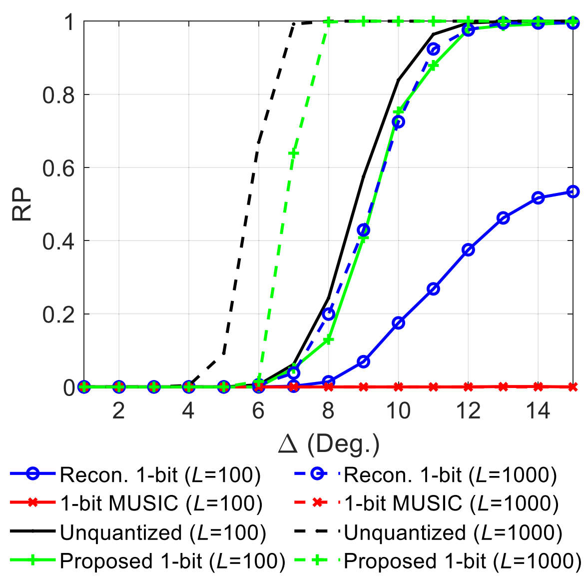

FIGURE 8. Comparison of RPs of various methods versus angular gap Δ.

the SNR of the second signal from -10 dB to 10 dB, the DOA of the second source is also variable (between 2.5 and 4.5 degrees). DOA and SNR of the first signal are still fixed. It is still observed that, in general, the proposed approach, among the one-bit methods, has the closest performance to the unquantized data output. It can also be seen that generally increasing the spatial distance (increasing the angular gap between the sources) decreases the RMSE, which is reasonable.

In the last experiment, the resolution probabilities (RPs) [18] of the algorithms are compared. For this purpose, it is assumed that the true DOAs of the two sources are $\theta_1 = -10°$ and $\theta_2 = -10° + \Delta$, and have SNRs of 10 and −10 dB, respectively, where $\Delta \in [1°, 15°]$ represents the angular gap between the two sources. In each independent run, it is assumed that the test is successful if the estimation errors of both DOAs are less than 0.5Δ (the middle angle of the two sources). Therefore, in the simulation, we have defined the RP as the ratio of the number of successful trials (N_S), to the total number of runs, i.e. $\mathrm{RP} \triangleq N_S / N_T$. The results are shown in Fig. 8. For both the number of snapshots equal to 100 and 1000, the proposed approach provided the best performance using one-bit measurements. Similar to the previous experiment, it can be seen that in fewer snapshots, the performance of the proposed approach is closer to the output of unquantized data. The more important point is that the RP values corresponding to the one-bit MUSIC algorithm, regardless of the number of snapshots, are always equal to zero, which means that the method [18], in a more practical scenario, where the powers of the signals are not necessarily equal, is absolutely not reliable.

V. CONCLUSION

In this paper, we first derived the GOBC matrix. Then, we highlighted the limitations of directly applying the one-bit covariance matrix, particularly in the presence of unbalanced SNRs, leading to the swapping of subspaces. Furthermore, we introduced a solution involving the smoothing of the GOBC matrix, significantly improving the final DOA estimation results. The presented analytical findings and numerical simulations demonstrated the efficacy of the proposed approach in overcoming practical challenges associated with unequal signal powers for one-bit DOA estimation. Comparative simulations with existing methods underscored the superiority of the proposed method, especially in scenarios with significant SNR differences and a limited number of snapshots. The research contributes a robust solution to enhance the reliability of one-bit DOA estimation in practical applications.

REFERENCES

[1] J. A. Zhang, M. L. Rahman, K. Wu, X. Huang, Y. J. Guo, S. Chen, and J. Yuan, "Enabling joint communication and radar sensing in mobile networks—A survey," *IEEE Commun. Surveys Tuts.*, vol. 24, no. 1, pp. 306–345, 1st Quart., 2022.

[2] A. M. Molaei, P. del Hougne, V. Fusco, and O. Yurduseven, "Efficient joint estimation of DOA, range and reflectivity in near-field by using mixed-order statistics and a symmetric MIMO array," *IEEE Trans. Veh. Technol.*, vol. 71, no. 3, pp. 2824–2842, Mar. 2022.

[3] Y. Tian, S. Liu, W. Liu, H. Chen, and Z. Dong, "Vehicle positioning with deep-learning-based direction-of-arrival estimation of incoherently distributed sources," *IEEE Internet Things J.*, vol. 9, no. 20, pp. 20083–20095, Oct. 2022.

[4] J. Wang, B. Shi, F. Shu, Q. Zhang, D. Wu, Q. Jie, Z. Zhuang, S. Feng, and Y. Zhang, "DOA estimation using massive receive MIMO: Basic principle and key techniques," 2021, *arXiv:2109.00154*.

[5] L. Zhang, C. Shi, J. Niu, Y. Ji, and Q. M. Jonathan Wu, "DOA estimation for HFSWR target based on PSO-ELM," *IEEE Geosci. Remote Sens. Lett.*, vol. 19, pp. 1–5, 2022.

[6] G. Jenkinson, M. A. B. Abbasi, A. M. Molaei, O. Yurduseven, and V. Fusco, "Deep learning-enabled improved direction-of-arrival estimation technique," *Electronics*, vol. 12, no. 16, p. 3505, Aug. 2023.

[7] A. Shastri, N. Valecha, E. Bashirov, H. Tataria, M. Lentmaier, F. Tufvesson, M. Rossi, and P. Casari, "A review of millimeter wave device-based localization and device-free sensing technologies and applications," *IEEE Commun. Surveys Tuts.*, vol. 24, no. 3, pp. 1708–1749, 3rd Quart., 2022.

[8] M. R. Dinčić, Z. H. Perić, D. B. Denić, and Z. Stamenković, "Design of robust quantizers for low-bit analog-to-digital converters for Gaussian source," *J. Circuits, Syst. Comput.*, vol. 28, Dec. 2019, Art. no. 1940002.

[9] A. B. L. B. Fernandes, Z. Shao, L. T. N. Landau, and R. C. de Lamare, "Comparator network aided detection for MIMO receivers with 1-bit quantization," in *Proc. 54th Asilomar Conf. Signals, Syst., Comput.*, Nov. 2020, pp. 384–387.

[10] L. V. Nguyen, A. L. Swindlehurst, and D. H. N. Nguyen, "Linear and deep neural network-based receivers for massive MIMO systems with one-bit ADCs," *IEEE Trans. Wireless Commun.*, vol. 20, no. 11, pp. 7333–7345, Nov. 2021.

[11] S. Sedighi, B. S. Mysore R, M. Soltanalian, and B. Ottersten, "On the performance of one-bit DoA estimation via sparse linear arrays," *IEEE Trans. Signal Process.*, vol. 69, pp. 6165–6182, 2021.

[12] S. Sedighi, M. R. B. Shankar, M. Soltanalian, and B. Ottersten, "DoA estimation using low-resolution multi-bit sparse array measurements," *IEEE Signal Process. Lett.*, vol. 28, pp. 1400–1404, 2021.

[13] S. Ge, C. Fan, J. Wang, and X. Huang, "Low-complexity one-bit DOA estimation for massive ULA with a single snapshot," *Remote Sens.*, vol. 14, no. 14, p. 3436, Jul. 2022.

[14] C.-L. Liu and P. P. Vaidyanathan, "One-bit normalized scatter matrix estimation for complex elliptically symmetric distributions," in *Proc. IEEE Int. Conf. Acoust., Speech Signal Process. (ICASSP)*, May 2020, pp. 9130–9134.

[15] S. Sedighi, B. Shankar, M. Soltanalian, and B. Ottersten, "One-bit DoA estimation via sparse linear arrays," in *Proc. IEEE Int. Conf. Acoust., Speech Signal Process. (ICASSP)*, May 2020, pp. 9135–9139.

[16] Y. Chen, C. Wang, and Y. Gao, "Classification-based one-bit DOA estimation for sparse arrays," *IEEE Access*, vol. 8, pp. 204891–204901, 2020.

[17] Z. Wei, W. Wang, F. Dong, and Q. Liu, "Gridless one-bit direction-of-arrival estimation via atomic norm denoising," *IEEE Commun. Lett.*, vol. 24, no. 10, pp. 2177–2181, Oct. 2020.

[18] X. Huang and B. Liao, "One-bit MUSIC," *IEEE Signal Process. Lett.*, vol. 26, no. 7, pp. 961–965, Jul. 2019.

[19] A. M. Molaei, B. Zakeri, and S. M. H. Andargoli, "Efficient clustering of non-coherent and coherent components regardless of sources' powers for 2D DOA estimation," *Circuits, Syst., Signal Process.*, vol. 40, no. 2, pp. 756–771, Feb. 2021.

[20] O. Bar-Shalom and A. J. Weiss, "DOA estimation using one-bit quantized measurements," *IEEE Trans. Aerosp. Electron. Syst.*, vol. 38, no. 3, pp. 868–884, Jul. 2002.

[21] S. Sun and Z. Ye, "Robust adaptive beamforming based on a method for steering vector estimation and interference covariance matrix reconstruction," *Signal Process.*, vol. 182, May 2021, Art. no. 107939.

[22] P. Wang, H. Yang, and Z. Ye, "1-bit direction of arrival estimation via improved complex-valued binary iterative hard thresholding," *Digit. Signal Process.*, vol. 120, Jan. 2022, Art. no. 103265.

[23] B. Fesl, M. Koller, and W. Utschick, "On the mean square error optimal estimator in one-bit quantized systems," *IEEE Trans. Signal Process.*, vol. 71, pp. 1968–1980, 2023.

[24] F. Santana and R. Santiago, "A generalized distance based on a generalized triangle inequality," *Inf. Sci.*, vol. 345, pp. 106–115, Jun. 2016.

[25] R. M. Howard, "Radial based approximations for arcsine, arccosine, arctangent and applications," *AppliedMath*, vol. 3, no. 2, pp. 343–394, Apr. 2023.

[26] N. Van Der Aa, H. Ter Morsche, and R. Mattheij, "Computation of eigenvalue and eigenvector derivatives for a general complex-valued eigensystem," *Electron. J. Linear Algebra*, vol. 16, pp. 300–314, 2007.

[27] K. Xu, M. Xing, R. Zhang, E. Hanyu, M. Sha, W. Nie, and Y. Quan, "High-accuracy DOA estimation algorithm at low SNR through exploiting a supervised index," *IEEE Trans. Aerosp. Electron. Syst.*, vol. 58, no. 4, pp. 3658–3665, Aug. 2022.
[28] M. A. Syed and M. Khalid, "Moving regression filtering with battery state of charge feedback control for solar PV firming and ramp rate curtailment," *IEEE Access*, vol. 9, pp. 13198–13211, 2021.
[29] W.-G. Tang, H. Jiang, and Q. Zhang, "One-bit gridless DOA estimation with multiple measurements exploiting accelerated proximal gradient algorithm," *Circuits, Syst., Signal Process.*, vol. 41, no. 2, pp. 1100–1114, Feb. 2022.
[30] C. Yang, C. Liu, and C. Shen, "Guided Gaussian range kernel filtering based on similarity-aware window," *J. Electron. Imag.*, vol. 31, no. 4, Jul. 2022, Art. no. 043022.
[31] A. M. Molaei, P. Del Hougne, V. Fusco, and O. Yurduseven, "Numerical-analytical study of performance of mixed-order statistics algorithm for joint estimation of DOA, range and backscatter coefficient in a MIMO structure," in *Proc. 23rd Int. Radar Symp. (IRS)*, Sep. 2022, pp. 396–401.

AMIR MASOUD MOLAEI (Member, IEEE) received the M.Sc. degree in telecommunication systems engineering from Sahand University of Technology, Tabriz, Iran, in 2013, and the Ph.D. degree in telecommunication systems engineering from Babol Noshirvani University of Technology (BNUT), Babol, Iran, in 2019.

He was ranked first in the Ph.D. entrance exam/interview in telecommunication systems with BNUT and ranked first among the Ph.D. graduates from the Telecommunication Engineering Department. From 2015 to 2019, he was a Lecturer with the Faculty of Electrical and Computer Engineering, BNUT. From 2019 to 2020, he was a Mobile Networks GSM/UMTS/LTE Analyzer and a Planner with Future Wave Ultratech Company, Tehran, Iran. Since 2020, he has been a Postdoctoral Research Fellow with the Centre for Wireless Innovation, School of Electronics, Electrical Engineering and Computer Science, Queen's University Belfast, Belfast, U.K. He has authored more than 50 refereed articles and has filed two patents. His current research interests include signal processing, radar imaging, and sensor arrays.

Dr. Molaei received the STAR Scheme Consolidated Performance Award for exceptional performance and contribution, in 2022 and 2023. He was the General Chair of the 2022 IEEE International Conference on Manufacturing, Industrial Automation and Electronics (ICMIAE). He was the Session Chair of the Passive and MIMO Radar Session at the 2022 IEEE 23rd International Radar Symposium (IRS). He is a Senior Editor of the *Cloud Computing and Data Science*. He has also served as a Technical Reviewer for numerous prestigious leading journals/magazines, including IEEE Wireless Communications, IEEE Transactions on Communications, and IEEE Journal of Selected Topics in Signal Processing.

VINCENT FUSCO (Fellow, IEEE) is currently the Director of Research with the ECIT Research Institute, Queen's University Belfast, Belfast, U.K. His fundamental work on active antenna front-end techniques has provided generic advances in low-cost phased and self-tracking antenna array architectures. He has authored or coauthored more than 500 articles and two books. He holds several antenna-related patents. He is a fellow of the Institution of Engineering and Technology and the Royal Academy of Engineering. He was a recipient of the IET Senior Achievement Award and Mountbatten Medal for seminal contributions to the field of microwave electronics and its impact on the U.K. industry, in 2012, and the 2019 Royal Irish Academy Gold Medal for Engineering Science.

OKAN YURDUSEVEN (Senior Member, IEEE) received the Ph.D. degree in electrical engineering from Northumbria University, Newcastle upon Tyne, U.K., in 2014.

Between 2018 and 2019, he was a NASA Research Fellow of the Jet Propulsion Laboratory, California Institute of Technology, USA. From 2014 to 2018, he was a Postdoctoral Research Associate with Duke University, USA. He is currently a Reader (Associate Professor) with the School of Electronics, Electrical Engineering and Computer Science, Queen's University Belfast, U.K. He has authored more than 200 peer-reviewed technical journals and conference papers. His research has been supported with extensive funding as a Principal Investigator and a Co-Investigator (in excess of £15 million). His research interests include microwave and millimetre-wave imaging, multiple-input-multiple-output (MIMO) radars, wireless power transfer, antennas and propagation, and metamaterials.

Dr. Yurduseven was a recipient of several awards, including an Outstanding Postdoctoral Researcher from Duke University Award, in 2017, Duke University Professional Development Award, in 2017, NASA Postdoctoral Program Award, in 2018, British Council—Alliance Hubert Curien Award, in 2019, Leverhulme Trust Research Leadership Award, in 2020 (£1M), Young Scientist Award from the Electromagnetics Academy—Photonics and Electromagnetics Research Symposium, in 2021, Queen's University Belfast Vice Chancellor's Early Career Researcher Prize, in 2022, and an Outstanding Associate Editor Award from the IEEE Antennas and Wireless Propagation Letters, in 2023. He serves as an Associate Editor for the IEEE Antennas and Wireless Propagation Letters and *Scientific Reports* (Nature) and a member for the European Association on Antennas and Propagation (EurAAP).